

# Forty years High Arctic climatological dataset of the Polish Polar Station Hornsund (SW Spitsbergen, Svalbard)

Tomasz Wawrzyniak, Marzena Osuch  
Institute of Geophysics, Polish Academy of Sciences, Warsaw, Poland  
*Correspondence to:* Tomasz Wawrzyniak (tomasz@igf.edu.pl)

**Abstract.** The article presents the climatological dataset from the Polish Polar Station Hornsund located in the southwest part of Spitsbergen - the biggest island of the Svalbard Archipelago. Due to a general lack of long-term in situ measurements and observations, the high Arctic remains one of the largest climate-data deficient regions on the Earth. Therefore, the described time series of observations in this paper are of unique value. To draw conclusions on the climatic changes in the Arctic, it is necessary to analyse and compare the long-term series of continuous, in situ observations from different locations, rather than relying on the climatic simulations only. In recent decades, rapid environmental changes occurring in the Atlantic sector of the Arctic are reflected in the data series collected by the operational monitoring conducted at the Hornsund Station. We demonstrate the results of the 40 years-long series of observations. Climatological mean values or totals are given, and we also examined the variability of meteorological variables at monthly and annual scale using the modified Mann-Kendall test for trend and Sen's method. The relevant daily, monthly, and annual data are provided on the PANGAEA repository (<https://doi.pangaea.de/10.1594/PANGAEA.909042>, Wawrzyniak and Osuch, 2019).

## 1 Introduction

For the analysis of the Arctic climate change, the long term operational monitoring of meteorological variables including reliable observations and measurements is obligatory. Weather conditions are crucial drivers that have feedback on many environmental components, and it is important to have a relevant dataset of atmospheric observation data if analysing the variability and fluctuations of climate at any given location. Climate change in the Arctic reflects a global warming trend, but the warming here is much faster than in lower latitudes (IPCC, 2019). The characteristics of Earth's climate zones are primarily determined by astronomical factors, but there are differences in the mechanisms that cause a regional warming trend and determine their magnitude. The presence of solar radiation, modified by the degree of cloudiness and type of clouds is the main factor influencing the transfer of energy. In polar regions during the polar night, the sole source of energy is the dynamic advection of heat from the oceanic and atmospheric circulations with regional differences throughout the area. Mechanisms of

Arctic amplification are still not fully understood but include feedback of reduced summer albedo due to reduction of sea ice extent and snow cover loss, higher sea surface temperatures, an increase of atmospheric water vapour content, cloud conditions, and changes in atmospheric circulation (IPCC, 2019). The growing number of positive annual air temperature anomalies in the Arctic varies substantially within the region, with the strongest changes observed in the Atlantic sector (Przybylak, 2016). Here, the Greenland Sea to the West of Svalbard is dominated by the West Spitsbergen Current, carrying warm (3–6°C) and salty (>35‰) Atlantic waters towards the Fram Strait. In this region, this flow is over 200 km wide and strongly influences the air temperature in the SW Spitsbergen area, especially during the winter (Walczowski et al., 2017). The specific maritime and mild climatic conditions are also influenced by local and regional factors as sea ice cover and its distribution (Dahlke et al., 2020), the presence of glaciers, orography of the terrain, and location near the seashore. The climatic variables such as air temperature, humidity, and precipitation vary significantly across the archipelago (Nordli et al., 2014; Osuch and Wawrzyniak, 2017a) as well as around the Hornsund Fjord (Arażny et al., 2018). Long-term, high-quality, in-situ consistent meteorological observations have been collected at the Hornsund Station located at the northern shore of this fjord. Relatively to the other parts of the Arctic, air temperatures in Svalbard are the highest at this latitude and their observed changes are one of the largest on Earth (IPCC, 2019). There is evidence for anomalies and changes in recent years in Atlantic sector of the Arctic, along western Spitsbergen, including higher air temperature (Gjelten et al., 2016) and higher liquid precipitation (Osuch and Wawrzyniak, 2017a). These changes have many environmental implications, leading to prolongation of the ablation season (Osuch and Wawrzyniak, 2017b), the negative mass balance of glaciers (Van Pelt et al., 2019), and permafrost degradation (Wawrzyniak et al., 2016).

## 2 Study area

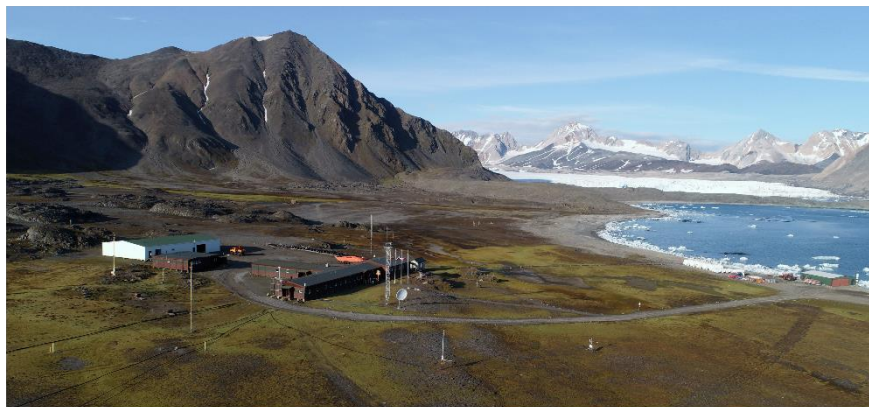
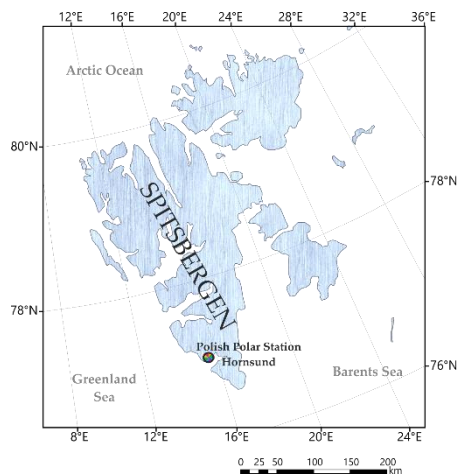


**Figure 1 Polish Polar Station Hornsund on Spitsbergen in the Svalbard Archipelago**

49 The Stanisław Siedlecki Polish Polar Station in Hornsund (77°00'N 15°33'E) located 300 m from the shore of Isbjørnhamna  
50 Bay of the Hornsund Fjord in SW Spitsbergen (Fig. 1), was established during the International Geophysical Year in 1957.  
51 Since 1978 it conducts year-round scientific research and is the northernmost permanent Polish scientific site, that throughout  
52 the years has become a modern interdisciplinary scientific platform that carries out research projects aimed at a better  
53 understanding of the functioning of the arctic nature and the changes it undergoes. The Hornsund Fjord is approximately 35  
54 km long and approximately 14.5 km wide at its mouth to the Greenland Sea. The coastline of Hornsund is diversified, with  
55 multiple bays and glaciated valleys. A recent expansion of the ice-free areas is observed in Svalbard, with the most significant  
56 retreats of the tidewater glaciers (Błaszczyk et al., 2013), so the recognition of the changes in the functioning of the  
57 environmental system becomes more and more essential. The station is set on a marine terrace at 10 m a.s.l.. This terrace,  
58 raised during Holocene (Lindner et al., 1991), consists of sea gravel and is covered by a diversity of tundra vegetation types.  
59 The slopes of the nearest mountain ranges Fugleberget (569 m) and Ariekammen (517 m) are located 1 km north from the  
60 station. Around 800 m NE from the station lies the lateral moraine of Hansbreen glacier. Recently the distance from the station  
61 to the front of Hansbreen is around 2.5 km. The ground here has a continuous permafrost layer down to more than 100 m deep  
62 (Wawrzyniak et al., 2016).

63 At Hornsund meteorological site indexed by international numbering system 01003 ([www.oscar.wmo.int](http://www.oscar.wmo.int)), managed by the  
64 Institute of Geophysics Polish Academy of Sciences, since July 1978 year-round, systematic, continuous measurements and  
65 observations at WMO standards have been conducted. The results of automatic measurements and visual observations are sent  
66 as the SYNOP-code to WMO database every 60 minutes and 3 hours, respectively. Since January 2001 most of the traditional  
67 instruments were replaced by an automatic weather station with Vaisala QLC-50 logger. The sensors of the new system have  
68 been installed on meteorological mast, situated 160 m SW of the main station building. To replace Vaisala QLC-50 in  
69 September 2016 new system Vaisala MAWS 301 was set on the same meteorological mast. To determine the degree of  
70 compatibility and homogeneity of the measurements, the old and new sensors were operating simultaneously for more than  
71 one year. The results of the analysis allowed to combine time series and since January 2018 the data comes from Vaisala  
72 MAWS 301. A comprehensive description of measurements and instruments can be found in collective work edited by Marsz  
73 and Styszyńska (2013) and in Table 1. Although the time series of the data stretches up to July 1978, here we analyse the  
74 variability of climatic conditions over the period 1979–2018 and in some cases 1983–2018, based on the availability of  
75 observations without gaps. The daily, monthly, and annual averages or sums and the extreme range (min and max), computed  
76 from observations are provided in the scientific digital data repository - PANGAEA (Wawrzyniak and Osuch, 2019).

### 77 **3 Meteorological variables**

78 Inter-seasonal weather fluctuations are determined by the changing Arctic climate system and atmospheric circulation. The  
79 changing global climate also modifies regional conditions. Weather conditions are crucial factors that have local feedback on  
80 many environmental components. Meteorological variables collected at the Hornsund Station help to characterise the climate

81 variability in this part of the Arctic and for a long time have been the background for multiple studies conducted in the SW  
82 Spitsbergen (Osuch and Wawrzyniak, 2017b, Wawrzyniak et al., 2017). Due to the diurnal variability of all meteorological  
83 variables, in this study, we use descriptive statistic methods to present the course and variation of multiple parameters. For  
84 most meteorological parameters, monthly mean values are calculated from daily mean values which are retrieved using the 3-  
85 hourly values (eight values a day, between 00:00 and 21:00 UTC); in case of precipitation 6-hourly values (12:00, 18:00, and  
86 00:00, 06:00 UTC of the following day); and daily sum of total solar radiation from Campbell–Stokes recorder obtained at the  
87 midnight.

88

89 **Table 1 Meteorological data measured at Hornsund including variables, current sensors, the period of operation, height, units, and**  
90 **their annual averages or sums.**

Variable	Location	Sensor	Period of operation	Height	Unit	Mean/sum
Air temperature (TA)	77°00'1.261" N 15°32'12.267" E	Traditional thermometer in Stevensons screen, Vaisala HMP 45D (since Jan 2001), HMP155 (since Jan 2018)	1979-2018	2 m agl	[°C]	TAm <sub>ax</sub> =-1.3 TAm <sub>ean</sub> =-3.7 TAm <sub>in</sub> =-6.0
Relative humidity (RH)	77°00'1.261" N 15°32'12.267" E	Hygrometer, HMP45D (since Jan 2001), HMP155 (since Jan 2018)	1979-2018 with gap 01.07.1982-16.08.1982	2 m agl	[%]	79.7
Precipitation	77°00'5.734" N 15°32'17.077" E	Hellmann Rain Gauge D-200	1979-2018	1 m agl	[mm]	478
Atmospheric pressure (PA)	77°00'1.261" N 15°32'12.267" E	Mercury barometer, PTB200A (since Jan 2001), Baro-1QML-AV (since Jan 2018)	1983-2018	Reduced to the sea level	[hPa]	1008.7
Wind speed (WS) and direction (WD)	77°00'1.261" N 15°32'12.267" E	Fuess 90z wind meter, Vaisala WAA151 (since Jan 2001), Vaisala WMT702 (since Jan 2018)	1983-2000 2001-2016 2017-2018	10 m agl	[m/s]	5.5
Sunshine duration (SD)	77°00'5.935" N 15°32'14.3" E	Campbell–Stokes Heliograph	1979-2018	2 m agl	[h]	1030.8

Cloudiness	On location	Visual observations	1983-2018		[octas]	5.85
Visibility	On location	Visual observations	1983-2018		[marine scale]	7.40

### 3.1 Air temperature

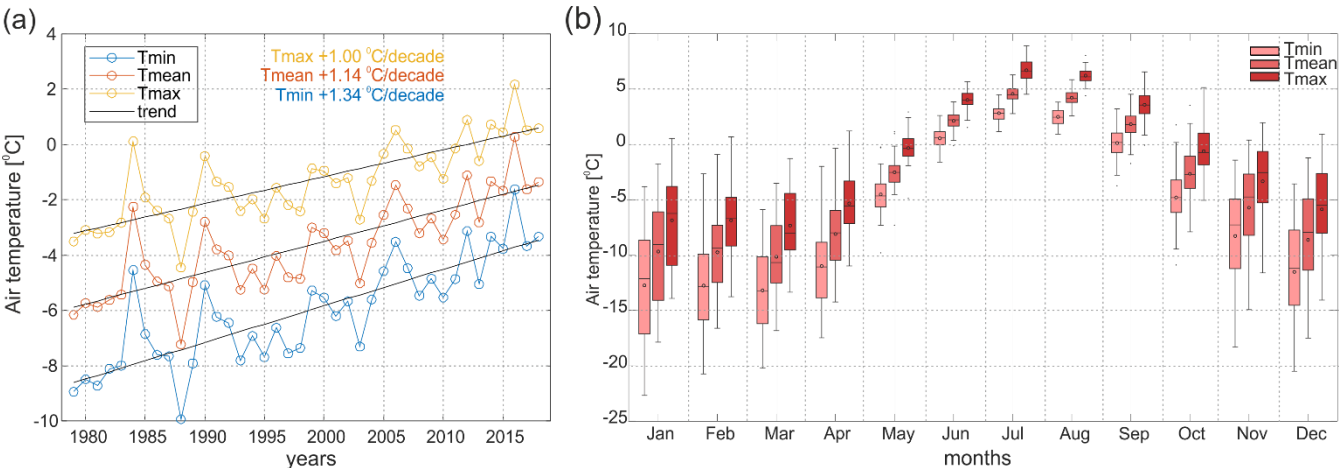
Air temperature (TA) can be presumed to be one of the most sensitive indicators of climatic changes. The time series of daily TA from the Hornsund Station covers the period 1979 to 2018. In the case of daily mean TA, there are no gaps in data while for maximum and minimum daily TA data for 01.09.1979, 29.02.1980, 15.06.2012, and 19.06.2017 are missing. Figure 2a presents the variability of the annual mean of minimum, mean, and maximum TA in 1979-2018 at the Hornsund Station. An upward trend is clearly visible for the three analysed variables. The significance of the trend was estimated by the modified Mann-Kendall test (Mann, 1945; Kendall, 1975; Hamed and Rao, 1998) taking into account autocorrelation of time series. The slope of the trend was estimated using Sen's method (Sen, 1968), where the slope is calculated as a median of the slopes of all pairs of points. The outcomes of the modified Mann-Kendall indicated that the trends are statistically significant; the estimated p-value is very small (less than  $1e-07$ ) for three presented variables.

The estimated slope of trend equal to 1.34, 1.14, and  $1.00^{\circ}\text{C}/\text{decade}$  for minimum, mean, and maximum TA respectively. These are one of the highest increases of mean TA on the planet, more than six times larger than the global average of  $+0.17^{\circ}\text{C}$  per decade (NOAA, 2020). The rest of the world is not expected to experience such changes until the end of this century (Hanssen-Bauer et al., 2019). The results of trend analyses for mean monthly TA (min, mean, and max) are presented in Table 2. In almost all months there are statistically significant trends except March. In all analysed cases the estimated slope of trend has positive values and indicated the increase in TA. A comparison of the results between variables shows that the largest changes were found for minimum daily TA ( $1.34^{\circ}\text{C}/\text{decade}$ ) while the lowest for the maximum daily TA ( $1.0^{\circ}\text{C}/\text{decade}$ ). Taking into account changes between months, the largest changes were estimated for January, February, and December (larger than  $2.0^{\circ}\text{C}/\text{decade}$  for minimum and mean daily TA). The smallest statistically significant are trends in July and August with slopes of the trend around  $0.3^{\circ}\text{C}/\text{decade}$ .

Figure 2b shows the boxplots of monthly averages of minimum, mean and maximum daily TA from the period 1979-2018. The variability of TA depends on the season, with the highest amplitudes during winter months. Summer TA is rather constant, with monthly means reaching usually slightly below  $5.0^{\circ}\text{C}$ . Average monthly TA during winter and early spring usually drop below  $-10.0^{\circ}\text{C}$ . The results are in general accordance with observations made at other arctic stations and reveal that winter is characterised by the highest variability of TA (Gjelten et al., 2016; Osuch and Wawrzyniak, 2017a). The amplitude between the extreme high and low in this season may be several times higher than in summer. These fluctuations are determined by the relatively stable anticyclonic subsidence with extreme cold and the turbulent cyclonic disturbances that bring higher temperatures, greater cloudiness, and heavy precipitation. The lowest recorded TA measured at a 2 m height above solid ground at Hornsund Station was  $-35.9^{\circ}\text{C}$  on 16.01.1981, while the absolute maximum  $15.6^{\circ}\text{C}$  on 31.07.2015. Mean annual air temperature (MAAT) in long-term 1979-2018 is  $-3.7^{\circ}\text{C}$ . The average coldest month is March with mean TA  $-10.2^{\circ}\text{C}$ , and on

121 the average warmest month is July with the mean TA of 4.6°C. The coldest month on record with mean -17.9°C was January  
122 1981, and the warmest July 2016 with mean 6.3°C. Additionally, in the data set we also provided monthly and annual positive  
123 (PDD) and negative degree days (NDD), calculated as the sum total of daily mean temperatures above or below the 0°C  
124 respectively.

125



126

127 **Figure 2 (a) Variability of an annual mean of min, mean, and max air temperatures in 1979-2018. (b) Variability of the monthly**  
128 **mean of min, mean, and max air temperatures in 1979-2018. On each box, the central line indicates the median, the circle represents**  
129 **the mean, and the bottom and top edges of the box indicate the 25th and 75th percentiles, respectively. The whiskers extend to the**  
130 **most extreme data points are not considered as outliers, and the outliers are plotted individually as dots.**

131 **Table 2 The slope of the trend in monthly and annual data (air temperature TA, relative humidity RH, precipitation Precip,**  
132 **atmospheric pressure at sea level PA, wind speed WS, wind direction WD, estimated by Sen's method in the period 1979-2018 for**  
133 **air temperature and sunshine duration and in 1983-2018 for other variables. The results of trend analysis by modified Mann-Kendall**  
134 **method to account for autocorrelation in the time series. Bold numbers denote statistically significant trend at the 0.05 level.**

month	TAmin [°C/dec]	TAmean [°C/dec]	TAmax [°C/dec]	RH [%/dec]	Precip [mm/dec]	PA [hPa/dec]	WS [m/decs]	SD [h/dec]	Cloudiness [octas/dec]	VV [-/dec]
JAN	<b>2.70</b>	<b>2.29</b>	<b>1.86</b>	-0.33	<b>3.51</b>	<b>1.54</b>	-0.14	0.00	0.12	-0.03
FEB	<b>2.46</b>	<b>2.14</b>	<b>1.74</b>	-0.41	1.48	<b>0.50</b>	0.06	<b>1.38</b>	-0.01	-0.06
MAR	0.74	0.57	<b>0.34</b>	<b>-1.13</b>	-1.61	<b>-0.27</b>	-0.13	5.52	0.04	<b>0.15</b>
APR	<b>1.37</b>	<b>1.00</b>	<b>0.79</b>	-0.64	-0.41	<b>-0.66</b>	-0.12	2.36	0.16	0.11
MAY	<b>0.97</b>	<b>0.70</b>	<b>0.49</b>	-0.27	1.92	<b>-0.10</b>	<b>0.40</b>	-10.07	0.00	-0.06
JUN	<b>0.61</b>	<b>0.52</b>	<b>0.54</b>	<b>-0.65</b>	-3.23	<b>0.27</b>	0.23	-1.80	0.11	0.13
JUL	<b>0.36</b>	<b>0.27</b>	<b>0.31</b>	0.26	1.11	<b>0.67</b>	0.12	-5.92	0.12	-0.07
AUG	<b>0.37</b>	<b>0.33</b>	<b>0.33</b>	0.00	7.49	<b>0.30</b>	0.09	5.18	0.02	-0.02
SEP	<b>0.73</b>	<b>0.67</b>	<b>0.62</b>	0.62	<b>19.67</b>	<b>0.18</b>	<b>0.50</b>	-1.33	0.16	-0.10

OCT	<b>1.16</b>	<b>1.07</b>	<b>1.01</b>	<b>1.50</b>	<b>13.53</b>	<b>1.15</b>	0.05	0.79	0.28	-0.08
NOV	<b>1.73</b>	<b>1.46</b>	<b>1.37</b>	0.30	5.43	<b>-0.60</b>	0.24	0.00	<b>0.26</b>	<b>-0.17</b>
DEC	<b>2.56</b>	<b>2.39</b>	<b>2.18</b>	0.18	5.24	<b>-0.95</b>	-0.06	0.00	<b>0.13</b>	-0.10
annual	<b>1.34</b>	<b>1.14</b>	<b>1.00</b>	0.10	<b>61.60</b>	<b>0.25</b>	0.08	-8.39	<b>0.12</b>	-0.02

### 3.2 Air humidity

The water vapour drives multiple atmospheric processes and has a significant influence on the global climate. It is the main greenhouse gas, affecting surface by feedback cycle through changing energy balance through radiative fluxes and cloud formation. According to general concepts, the Arctic warming of recent decades is accompanied by the hydrological cycle intensification (Vihma et al., 2015). To understand the variability of water vapour concentration and its causes is highly important, especially for climate studies as well as in water balance calculations. At the Hornsund Station, the air humidity is measured recently by sensor HMP155 that replaced the previously used HMP45D sensor. The observations cover period 1979-2018, but measurements were performed four times a day (0, 6, 12, 18 UTC) within the periods: 1.07.1978-26.07.1981 and 16.08.1982-31.07.1986, two times a day (6 and 18 UTC) from 27.07.1981 to 30.06.1982, eight times a day (0, 3, 6, 9, 12, 15, 18, 21 UTC) since 1.08.1986. Daily time series of the relative humidity (RH) was calculated as a mean of all available measurements within a particular day. There is a gap in the measurements from 01.07.1982 to 15.08.1982. Therefore the trend analyses were performed for the period 1983-2018.

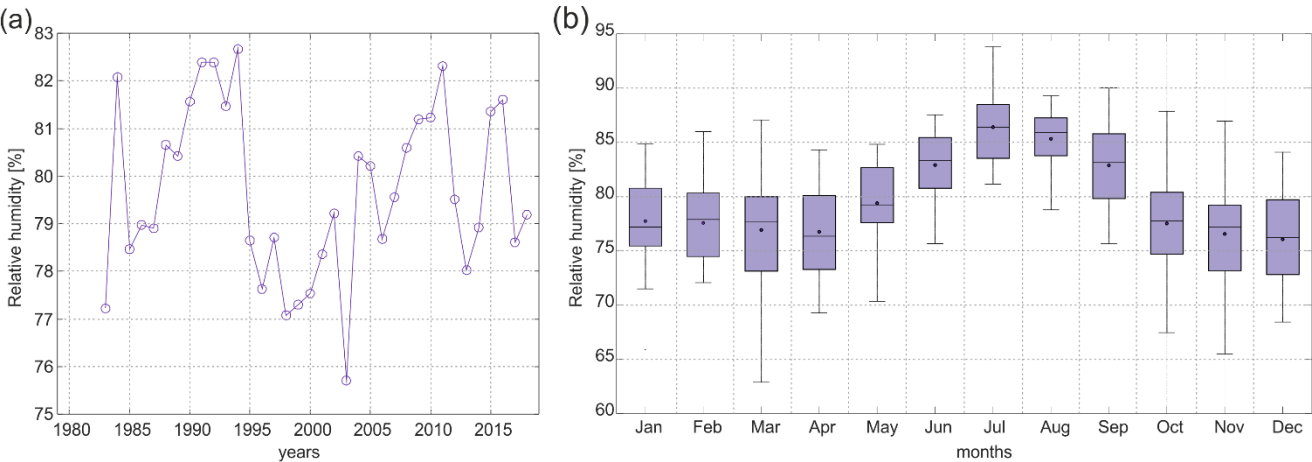


**Figure 3 (a) Variability of an annual mean of relative humidity in 1983-2018 at Hornsund. (b) Variability of mean monthly relative humidity in 1983-2018 at Hornsund.**

151 The variability of the annual mean RH in the period 1983-2019 is presented in Figure 3a. The average over the period 1983-  
152 2018 is 79.7%. The range of variability is from 75.7% (2003) to 82.7% in 1994. The trend analyses indicated a statistically  
153 insignificant trend.

154 The course of the monthly mean RH in the period 1983-2018 is presented in Figure 3b. Higher values of mean RH are observed  
155 in warmer months of the year and lower during winter. Such high values are attributed to continual dominance of marine air  
156 masses. The annual course of the RH is strongly connected with the air temperature and shows typical variability. It generally  
157 increases with warmer air temperatures. However, most of the trends are not statistically significant at the 0.05 level except  
158 March, June, and October.

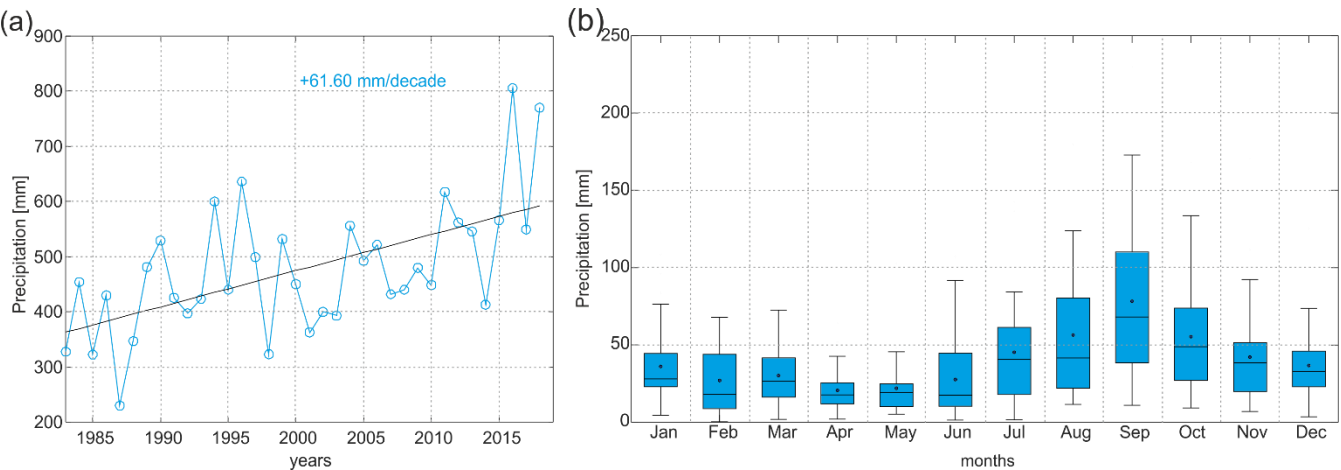
159 The analyses at daily time scale indicated that drops of RH below 50% are recorded rather sporadically, although these can  
160 occur throughout the year. Such situations are connected with advection of strongly cooled air masses, foehn effects, or  
161 katabatic winds from Hansbreen (Marsz and Styszyńska, 2013). The minimum observed quantity reached 24% on 15.01.1981.  
162 The maximum of the observed RH is equal to 100%. Such conditions occurred 27 times in the period 1979-2018.

### 163 **3.3 Precipitation**

164 In the case of precipitation, the daily sum at the Hornsund Station is calculated from four measurements obtained from  
165 unfenced Hellmann Rain Gauge at 12:00, 18:00, and 00:00, 06:00 of the following day, with the orifice 200 cm<sup>2</sup>, placed 1 m  
166 above the ground level. The time series of the daily sum of precipitation cover period 1979-2018 with the gap in July 1982.

167 The influence of the West Spitsbergen Current creates a relatively moist climate in SW Spitsbergen region, which is clearly  
168 reflected in the amount of precipitation. In comparison to the other meteorological stations in Spitsbergen (Osuch and  
169 Wawrzyniak, 2017a; Hanssen-Bauer et al., 2019), the annual amount reaching 477 mm is the highest. The variability of the  
170 annual sums of precipitation in the period 1983-2018 is shown in Figure 4a. The amount of precipitation varies from 230 mm  
171 in 1987 to 805.5 mm in 2016. The trend analyses indicated large changes, an increase of 61.6 mm/decade for the annual sums  
172 of precipitation.





174

175 **Figure 4 (a) Variability of annual sums of precipitation in 1983-2018 at Hornsund. (b) Variability of mean monthly sums of**  
176 **precipitation in 1983-2018 at Hornsund.**

177 The annual course of monthly sums of precipitation from the period 1983-2018 is presented in Figure 4b. The driest months  
178 are April and May with the average 23 and 24 mm respectively. The highest precipitation is recorded in September reaching  
179 on average 75 mm. Trend analyses presented in Table 2 indicated statistically significant changes in January (3.51 mm/decade),  
180 September (19.67 mm/decade), and October (13.53 mm/decade).

181 **3.4 The atmospheric pressure**

182 The measurements of the atmospheric pressure (PA) at Hornsund started in July 1978. In the beginning, PA was measured  
183 with a mercury barometer every 3 hours. Since 2001 measurements have been conducted every 60 seconds with a Vaisala  
184 PTB200A sensor, replaced by BARO-1QML\_AV in 2018. The lowest recorded PA reduced to sea level at Hornsund Station  
185 was 982.2 hPa on 30.08.1994, while the absolute maximum 1028.5 hPa on 07.08.1987. Mean annual PA in long-term 1983-  
186 2018 is 1008.7 hPa and its variability is presented in Figure 5a. It is visible an increasing trend (0.25 hPa /decade) but  
187 statistically insignificant (pval>0.05).

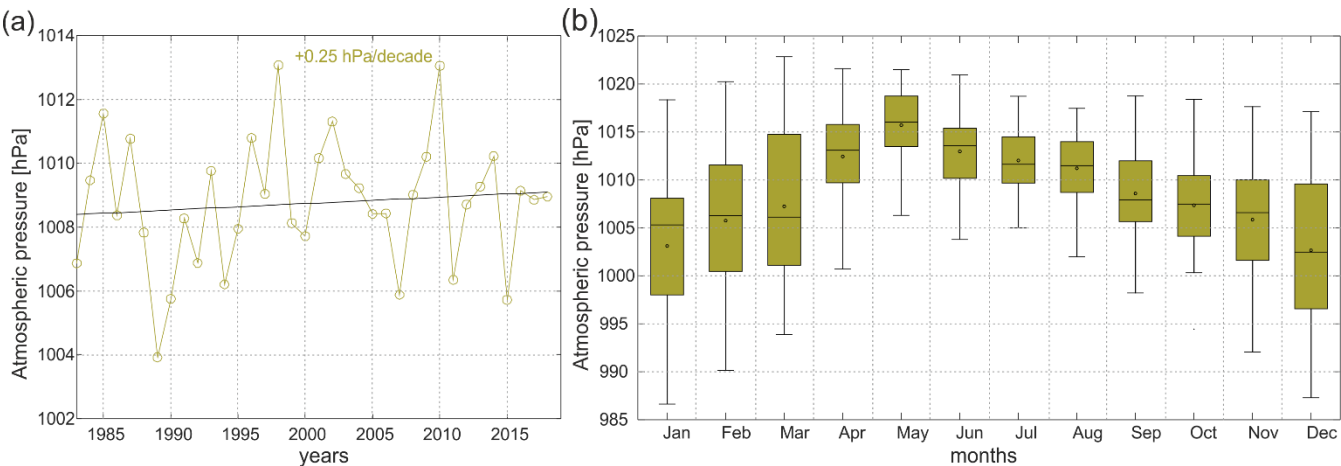
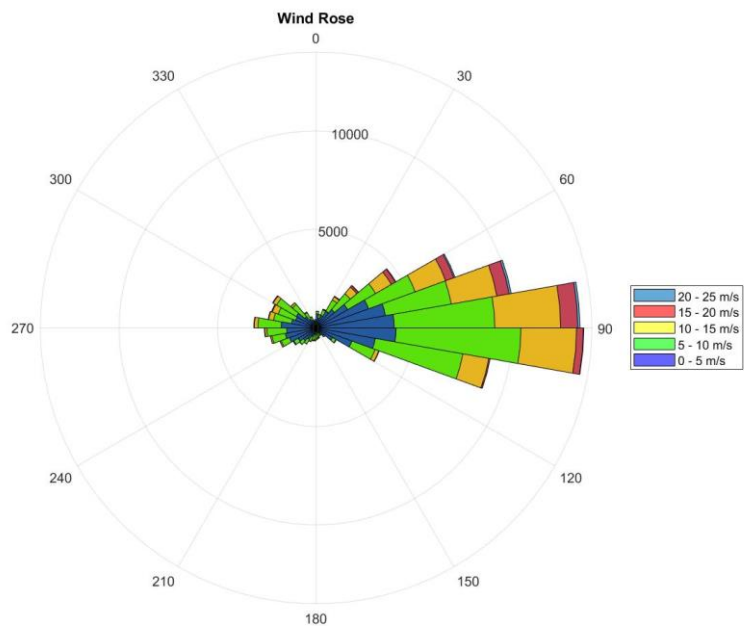


**Figure 5 (a) Variability of mean annual air pressure reduced to sea level in 1983-2018 at Hornsund. (b) Variability of mean annual air pressure reduced to sea level in 1983-2018 at Hornsund.**

Figure 5b shows the variability of the mean monthly PA over period 1983-2018. Well pronounced seasonality is visible, with mean monthly pressure higher than 1010 hPa from April to August. The month with the lowest mean PA is December with mean 1002.7 hPa, and the month with the largest PA is May with the mean of 1015.7 hPa. The variability of mean monthly PA within the observation period also is visible with the largest variability in January and February (larger than 30 hPa) and the smallest in July (13.7 hPa). The trend analyses of mean monthly PA resulted in statistically insignificant trend for all months.

### 3.5 Wind speed and direction

The wind is a result of atmospheric circulation and is highly correlated with the intensity of cyclonic activity (Przybylak 2016). The wind regime results from the latitudinal shape of the Hornsund fjord, location near the seashore and local topography. The measurements of wind speed (WS) and wind direction (WD) were performed at Hornsund with different sensors: 1978-2000 with the Fuess 90z wind meter, 2001-2017 with Vaisala WAA151 for direction and wind speed, since 2018 with Ultrasonic Wind Sensor WMT702. At Hornsund Station the height of the anemometer is 10 m above the ground, around 20 m above sea level. WS is measured with an accuracy of 0.1 m/s and WD with 5°. The wind rose for the Hornsund station is presented in Figure 6. Winds blowing from the East, along the fjord, are prevailing.

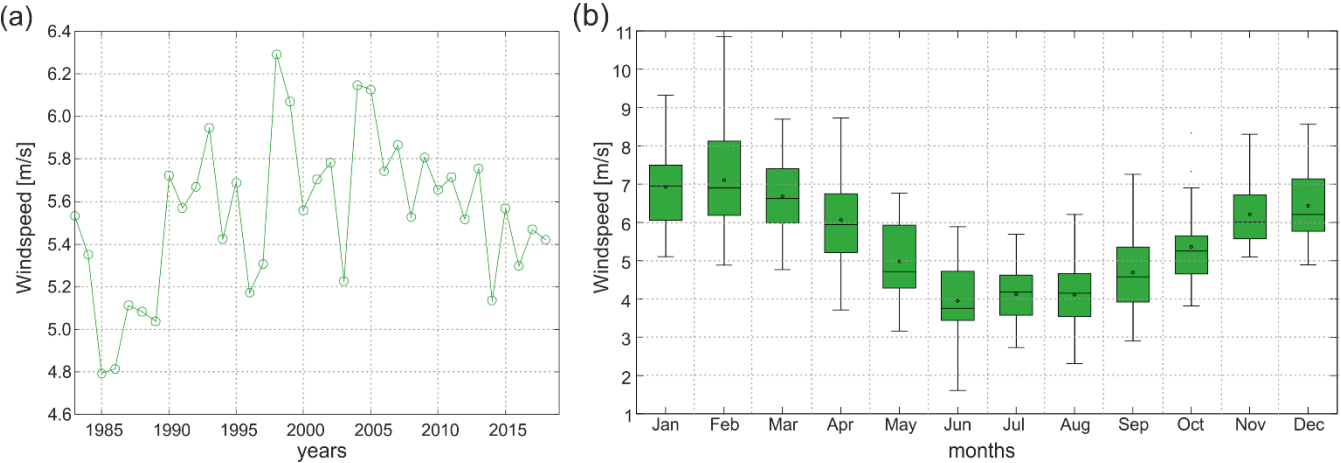


207

208 **Figure 6 The wind rose for the Hornsund station for the period 1983-2018.**

209 The variability of the mean annual WS at Hornsund in the period 1983-2018 is shown in Figure 7a. The average over the  
210 period 1983-2018 is equal to 5.5 m/s. The lowest values of WS was observed in 1985 (4.8 m/s) while the largest in 1998 (6.3  
211 m/s). There is a statistically insignificant trend in mean annual WS.

212



213

214 **Figure 7 (a) Variability of mean annual wind speed in 1983-2018 at Hornsund. (b) Variability of the mean monthly wind speed at**  
215 **Hornsund in the period 1983-2018.**

216 The variability of mean monthly WS in the period 1983-2018 is presented in Figure 7b. WS regime is well visible with smaller  
 217 average values during summer months (minimum 4.0 m/s in June) and larger average values during winter (maximum 7.1 m/s  
 218 in February). Such variability is a result of the extreme cyclone events that often occur during arctic winters (Rinke et al.,  
 219 2017).

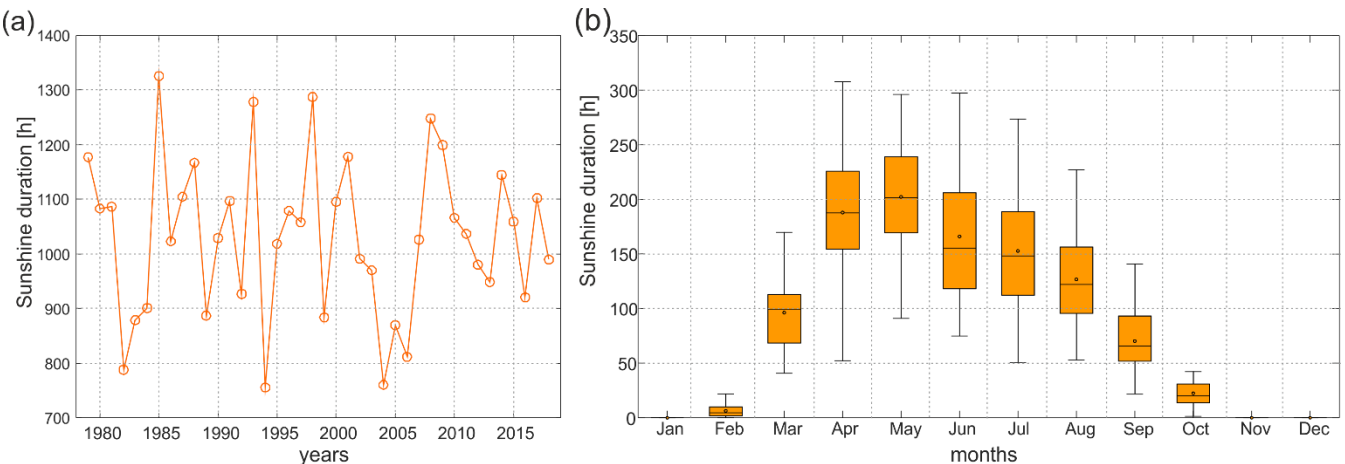
220 **3.6 Sunshine duration**

221 Sunshine duration (SD) is one of the important meteorological variables that provides data on the time period during which  
 222 direct solar radiation reaches the Earth’s surface and partly on the quantity of total solar energy. Daily SD is measured at  
 223 Hornsund using a Campbell-Stokes sunshine recorder (CS). It uses a direct optical method with the heat energy of the Sun’s  
 224 direct radiation burning the card. Such traditional sunshine recorder has been in service worldwide since the nineteenth century  
 225 and although there are multiple automatic radiometers used simultaneously at the Hornsund Station, the longest data is recorded  
 226 by CS. The time series of sunshine duration cover period 1983-2018. At the Hornsund Station, the polar night lasts 104 days  
 227 (October 31 – February 11), while the polar day lasts 117 days (April 24 – August 18).

228 Figure 8a shows the variability of the annual sums of SD at Hornsund in the period 1979-2018. The mean value is 1030.8 h  
 229 that is about 28% of the potential SD calculated for the station (Wojkowski et al., 2015). The large span in the annual SD is  
 230 visible. The minimum value (755.4 h) was observed in 1994 and maximum (1325.6 h) in 1985. The slightly decreasing trend  
 231 in SD is visible but statistically insignificant at the 0.05 level.

232

233



234 **Figure 8 (a) Variability of mean annual sunshine duration in 1979-2018 at Hornsund. (b) Variability of the monthly sums of sunshine**  
 235 **duration at Hornsund in the period 1979-2018.**  
 236

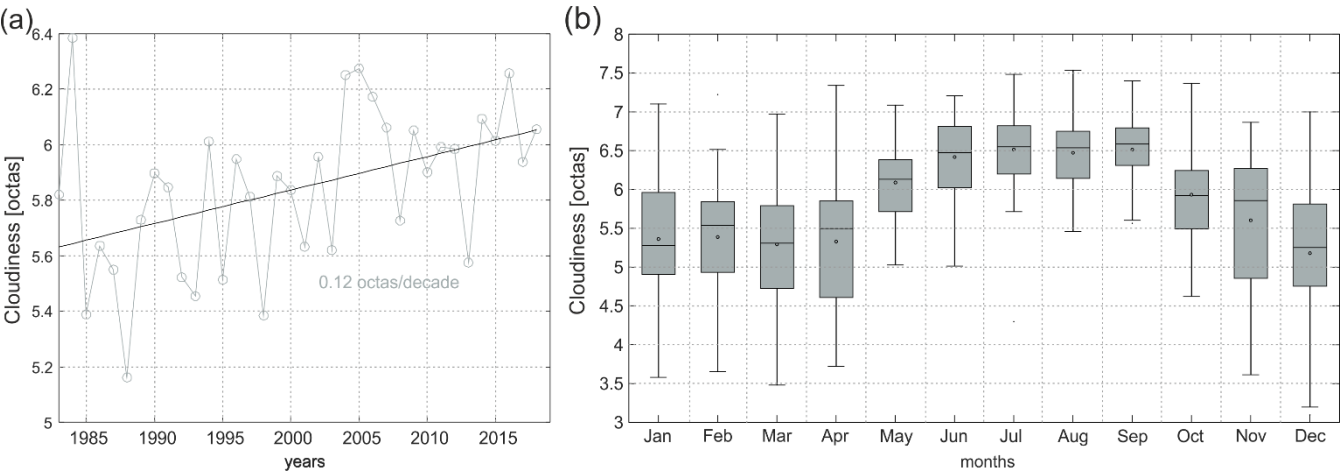
237 Monthly total SD is presented in Figure 8b. Its variability results from the different duration of the day at the location (latitude  
 238 77N) with zero SD during the polar night.

239 **3.7 Cloudiness**

240 Arctic clouds have a warming effect on the surface during most of the year because their effect of increasing the downward  
241 longwave radiation dominates their effect of reducing the net solar radiation over high-albedo snow and ice surfaces. In  
242 summer, however, clouds typically have a cooling effect on surface types with a lower albedo, such as the open sea, melting  
243 sea ice, and ground (Intrieri et al., 2002; Shupe and Intrieri, 2004). Observations of cloudiness at the Polish Polar Station in  
244 Hornsund are conducted by meteorologists and describe the predominant sky condition based upon octas (eighths) of the sky  
245 covered by opaque (not transparent) clouds. There are many factors that may hinder the heterogeneity and evaluation of  
246 cloudiness, due to the annual change in the meteorological observers and a fact that observers might be subjective, although  
247 are provided with clear observable criteria.

248 Annual averages of cloudiness in the period 1983-2018 is presented in Figure 9a. The mean over this period equals 5.85 octas.  
249 The minimum value of annual mean was observed in 1988 (5.16 octas) and maximum in 1984 (6.39 octas). An increasing  
250 tendency of mean annual cloudiness is visible. The estimated trend (slope 0.13 octas/decade) is statistically significant at the  
251 0.05 level.

252



253

254 **Figure 9 (a) Variability of mean annual cloudiness in 1983-2018 at Hornsund. (b) Variability of the monthly sums of cloudiness at**  
255 **Hornsund in the period 1983-2018.**

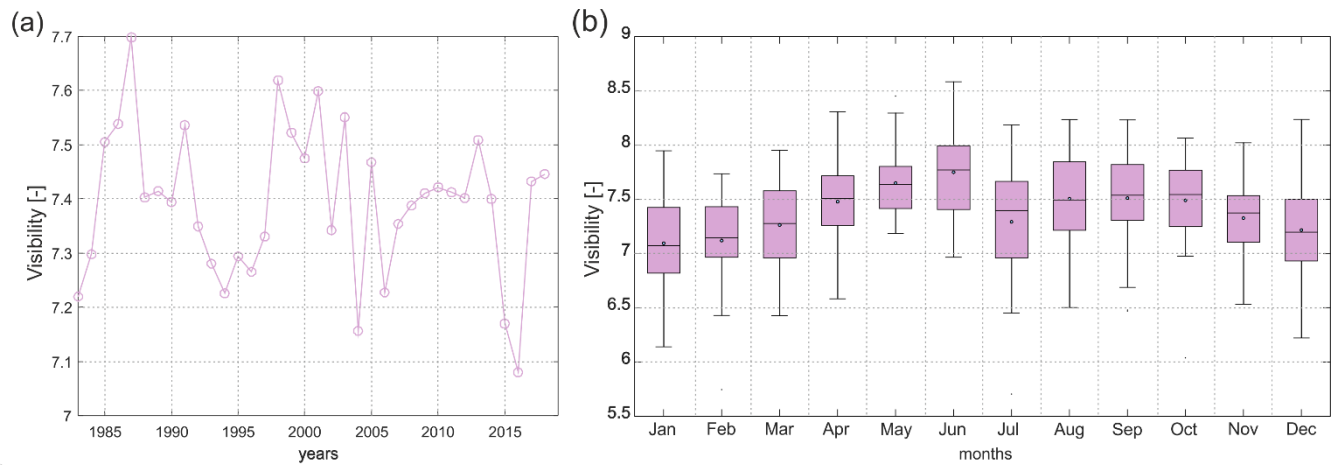
256 The variability of the monthly cloudiness in the period 1983-2018 is presented in Figure 9b. The annual cycle is characterised  
257 by lower mean cloudiness during the cold period from October till April (5.5-6.0 octas), and this period is also characterised  
258 by large inter-annual variability. The period from May till September is on the average more cloudy (6.0-6.7 octas) and inter-  
259 annual variability is lower.

260 **3.7 Visibility**

261 The horizontal visibility is quantified using observations made by meteorologists in the surroundings of the Hornsund Station  
262 with a marine scale that ranges from 1 to 9. The visual observations are performed using known distances to the surrounding  
263 mountains and other objects. Values 1 and 2 correspond to very bad visibility, 0-50 m and 50-200 m, respectively. Bad  
264 visibility (200 m – 1 km) is represented by value 3. Weak horizontal visibility represents conditions with 1-2 km and 2-4 km  
265 that are quantified as 4 and 5 in the applied scale. Moderate horizontal visibility, described as 6 in the scale, represent conditions  
266 when an object or light can be clearly discerned from 4-10 km. Good horizontal visibility (7 in the scale) is 10-20 km, very  
267 good (8) 20-50 km and extremely good (9) is for horizontal visibility larger than 50 km. Noted visibility might be reduced by  
268 multiple factors, including all products of the condensation of water vapour such as fog, precipitation, as well as darkness  
269 during cloudy conditions throughout the polar night, as there are no artificial lights in the area. There are no anthropogenic  
270 factors that would reduce visibility in the vicinity of the Hornsund Station as it is located in the middle of the strictly protected  
271 South Spitsbergen National Park. Due to that reduced visibility cannot be an indicator of poor air quality on the local scale.

272  
273 Figure 10a shows the variability of mean annual visibility in the period 1983-2018. On average in this period is good horizontal  
274 visibility that amounts 7.40; minimum mean annual visibility was observed in 2016 (7.08) while maximum in 1987 (7.70). A  
275 decreasing tendency is visible (slope of trend -0.02 per decade) however the trend is statistically insignificant at the 0.05 level.  
276 Variability of the mean monthly visibility at Hornsund in the period 1983-2018 is presented in Figure 10b. It is characterised  
277 by both low inter-annual and interseasonal variability and on average reaches values between 7 and 8.

278



279

280 **Figure 10 (a) Variability of mean annual visibility in 1983-2018 at Hornsund. (b) Variability of the mean monthly visibility at**  
281 **Hornsund in the period 1983-2018.**

## 282    **4 Quality control of the time series**

283    All presented datasets have undergone a thorough quality control process. Such process consisted of multiple steps as the  
284    measurements may not be homogenous due to the varying number of observations during the day, changes of sensors, and  
285    other factors (Estévez et al., 2011). In the first step, the data were visualised as a time series that allowed verification if all data  
286    have been collected and that the record structure is correct, complete, and without any gaps. In this way also the presence of  
287    outliers and step change in the data was tested. To determine the degree of compatibility and homogeneity of the measurements  
288    from different sensors, changed over years, the old and new sensors were operated simultaneously for more than one year. The  
289    results allowed to combine time series. In the following step, different variables were compared to test the internal consistency  
290    between variables. Such analyses include a comparison of minimum, mean, and maximum daily TA that follow the rule  
291     $T_{Amax} > T_{Amean} > T_{Amin}$ . In the case of WS and WD following conditions were tested  $WS=0$  and  $WD=0$ ,  $WS \neq 0$  and  $WD \neq 0$ .  
292    In the third step temporal consistency of time series was analysed with the help of statistical tests of homogeneity (Pettit and  
293    Standard Normal Homogeneity Test). In the last step, the same variables but from different meteorological stations in Svalbard  
294    were compared. The air temperature time series were tested against observations in Barentsburg, Bjørnøya, Hopen,  
295    Longyearbyen (Svalbard Lufthavn), Ny Ålesund, and Sveagruva. For that purpose, the data were visualised and checked with  
296    the Standard Normal Homogeneity Test (Alexandersson, 1986; Nordli et al., 1996). The applied algorithm showed good  
297    performance in both detecting breakpoints and identifying homogeneous time series. By application of the relative method,  
298    with comparison to the other available datasets from Svalbard, the gradual and step changes due to climate change were not  
299    found as a source of inhomogeneity.

## 300    **5 Data availability**

301    The dataset described in this article is available on the PANGAEA repository (Wawrzyniak and Osuch, 2019:  
302    <https://doi.pangaea.de/10.1594/PANGAEA.909042>).

## 303    **6 Summary**

304    This paper has presented details of a long-term (1979–2018) dataset from the meteorological site at the Polish Polar Station  
305    Hornsund located in the SW part of Spitsbergen. The data series includes daily, monthly and annual air temperature, PDD,  
306    NDD, the sum of precipitation, air humidity, atmospheric pressure, wind speed and direction, sunshine duration, cloudiness,  
307    and visibility. This rich dataset, now available online, is a valuable source for documenting the state of the climate in SW  
308    Spitsbergen that represents the Atlantic sector of the Arctic. With the positive trend of mean annual temperature  
309     $+1.14^{\circ}\text{C}/\text{decade}$  in the last four decades (1979–2018), the climate in Hornsund is warming in this period more than six times  
310    larger than the global average that amounts  $+0.17^{\circ}\text{C}$  per decade (NOAA, 2020). All climatological variables presented in this

study have many environmental implications and there are both broad scientific interest and societal need to understand climate variability and its influence on geoecosystems.

## 7 Author Contributions

TW and MO wrote the paper and carried out the data processing and analysis.

## 8 Competing Interests

The authors declare that they have no conflict of interest.

## Acknowledgements

The authors would like to kindly thank the meteorological staff from the Polish Polar Station Hornsund listed here: <https://hornsund.igf.edu.pl/about-the-station/expeditions/> for collecting the data and maintaining the meteorological monitoring. The authors also thank the two anonymous reviewers for valuable comments and suggestions. Financial support for this work was provided by the Polish National Science Centre through grant No. 2017/27/B/ST10/01269. This work was also partially supported by the Institute of Geophysics, Polish Academy of Sciences within statutory activities No 3841/E-41/S/2020 of the Ministry of Science and Higher Education of Poland.

## References

- Arażny, A., Przybylak, R., Wyszynski, P., Wawrzyniak, T., Nawrot, A., and Budzik, T.: Spatial variations in air temperature and humidity over Hornsund fjord (Spitsbergen) from 1 July 2014 to 30 June 2015, *Geografiska Annaler: Series A, Physical Geography*, 100(1), 27-43, doi: 10.1080/04353676.2017.1368832, 2018.
- Błaszczuk, M., Jania, J. A., and Kolondra, L.: Fluctuations of tidewater glaciers in Hornsund Fjord (Southern Svalbard) since the beginning of the 20th century, *Polish Polar Research*, 34(4), 327–352, doi:10.2478/popore-2013-0024, 2013.
- Dahlke, S., Hughes, N.E., Wagner, P.M., Gerland, S., Wawrzyniak, T., Ivanov, B., and Maturilli, M.: The observed recent surface air temperature development across Svalbard and concurring footprints in local sea ice cover. *Int J Climatol.*; 1– 20. <https://doi.org/10.1002/joc.6517>, 2020.
- Estévez, J., Gavilán, P., and Giráldez, J. V.: Guidelines on validation procedures for meteorological data from automatic weather stations. *Journal of Hydrology*, 402(1-2), 144–154, doi:10.1016/j.jhydrol.2011.02.031, 2011.
- Gjelten, H.M., Nordli, Øyvind, Isaksen, K., Førland, E.J., Sviashchennikov, P. N., Wyszynski, P., Prokhorova, U. V., Przybylak, R., Ivanov, B.V., and Urazgildeeva, A. V.: Air temperature variations and gradients along the coast and fjords of western Spitsbergen. *Polar Research*, 35. <https://doi.org/10.3402/polar.v35.29878>, 2016.



338 Hamed, K. H., and Rao, R.: A modified Mann-Kendall trend test for autocorrelated data, *J. Hydrol.*, 204, 182–196, 1998.

339 Hanssen-Bauer, I., Førland, E.J., Hisdal, H., Mayer, S., Sandø, A.B., Sorteberg, A., Adakudlu, M., Andresen, J., Beldring, S.,  
340 Benestad, R., Bilt, W., Bogen, J., Borstad, C., Breili, K., Breivik, Ø., Børsheim, K.Y., Christiansen, H.H., Dobler, A., Engeset,  
341 R., Frauenfelder, R., Gerland, S., Gjeltén, H.M., Gundersen, J., Isaksen, K., Jaedicke, C., Kierulf, H., Kohler, J., Li, H., Lutz,  
342 J., Melvold, K., Mezghani, A., Nilsen, F., Nilsen, I.B., Nilsen, J.E.Ø., Pavlova, O., Ravndal, O., Risebrobakken, B., Saloranta,  
343 T., Sandven, S., Schuler, T.V., Simpson, M.J.R., Skogen, M., Smedsrud, L.H., Sund, M., Vikhamar-Schuler, D., Westermann,  
344 S., Wong, W.K.: Climate in Svalbard 2100 – a knowledge base for climate adaptation. Norwegian Centre for Climate Services,  
345 Report no. 1/2019, ISSN 2387-3027, 205 pp., 2019.

346 Intrieri, J. M., Fairall, C. W., Shupe, M. D., Persson, P. O. G., Andreas, E. L., Guest, P., and Moritz, R. M.: An annual cycle  
347 of Arctic surface cloud forcing at SHEBA. *J. Geophys. Res.*, 107, 8039, doi:10.1029/2000JC000439, 2002.

348 IPCC: The Ocean and Cryosphere in a Changing Climate. <https://www.ipcc.ch/srocc/home/>, 2019.

349 Kendall, M. G.: Rank Correlation Methods. Charles Griffin: London, 1975.

350 Lindner, L., Marks, L., Roszczyński, W. and Semil, J.: Age of raised marine beaches of northern Hornsund Region, South  
351 Spitsbergen, *Pol. Polar Res.*, 12(2), 161-182, 1991.

352 Mann, H.: Nonparametric tests against trend, *Econometrica*, 13(3), 245–259, doi:10.2307/1907187, 1945.

353 Marsz, A. A., and Styszyńska, A.: Climate and Climate change at Hornsund, Svalbard. Gdynia Maritime University: Gdynia,  
354 Poland, ISBN: 978-83-7421-191-8, 2013.

355 NOAA National Centers for Environmental information, Climate at a Glance: Global Time Series, published February 2020,  
356 retrieved on February 27, 2020 from <https://www.ncdc.noaa.gov/cag/>, 2020.

357 Nordli, P. Ø., Hanssen-Bauer, I., and Førland, E. J.: Homogeneity Analyses of Temperature and Precipitation Series from  
358 Svalbard and Jan Mayen, Norwegian Meteorol. Inst. Report 16/96 KLIMA, 41, 1996.

359 Nordli, Ø., Przybylak, R., Ogilvie, A. E. J., and Isaksen, K.: Long-term temperature trends and variability on Spitsbergen: the  
360 extended Svalbard Airport temperature series, 1898–2012, *Polar Res.*, 33, 21349, doi: 10.3402/polar.v33.21349, 2014.

361 Osuch, M. and Wawrzyniak, T.: Climate projections in the Hornsund area, Southern Spitsbergen, *Pol. Polar Res.*, 37(3), 379–  
362 402, doi:10.1515/popore-2016-0020, 2016.

363 Osuch, M. and Wawrzyniak, T.: Inter- and intra-annual changes of air temperature and precipitation in western Spitsbergen,  
364 *Int. J. Climatol.*, 37, 3082–3097, doi:10.1002/joc.4901, 2017a.

365 Osuch, M. and Wawrzyniak, T.: Variations and changes in snow depth at meteorological stations Barentsburg and Hornsund  
366 (Spitsbergen), *Ann. Glaciol.*, 58 (75), 11–20, doi:10.1017/aog.2017.20, 2017b.

367 Osuch, M., Wawrzyniak, T., and Nawrot, A.: Diagnosis of the hydrology of a small Arctic permafrost catchment using HBV  
368 conceptual rainfall-runoff model, *Hydrology Research*, 50(2), 459-478, doi:10.2166/nh.2019.031, 2019.

369 Przybylak, R.: The climate of the Arctic. 2nd ed. Atmospheric and Oceanographic Sciences Library 52, Heidelberg: Springer;  
370 pp. 287, doi:10.1007/978-3-319-21696-6, 2016.

371 Rinke, A., M. Maturilli, R.M. Graham, H. Matthes, D. Handorf, L. Cohen, S.R. Hudson, and Moore, J.C.: Extreme cyclone  
 372 events in the Arctic: Wintertime variability and trends, *Envir. Res. Lett.*, 12, 094006, doi:10.1088/1748-9326/aa7def, 2017.  
 373 Sen, P. K.: Estimates of the regression coefficient based on Kendall's tau, *Journal of the American Statistical Association*, 63,  
 374 1379–1389, doi: 10.2307/2285891, 1968.  
 375 Shupe, M. D., and Intrieri, J. M.: Cloud radiative forcing of the Arctic surface: The influence of cloud properties, surface  
 376 albedo, and solar zenith angle. *J. Climate*, 17, 616–628, doi:10.1175/1520-044, 2004.  
 377 van Pelt, W., Pohjola, V., Pettersson, R., Marchenko, S., Kohler, J., Luks, B., Hagen, J. O., Schuler, T. V., Dunse, T., Noël,  
 378 B., and Reijmer, C.: A long-term dataset of climatic mass balance, snow conditions, and runoff in Svalbard (1957–2018), *The*  
 379 *Cryosphere*, 13, 9, 2259–2280, doi: 10.5194/tc-13-2259-2019, 2019.  
 380 Vihma, T., Screen, J., Tjernström, M., Newton, B., Zhang, X., Popova, V., Deser, C., Holland, M., and Prowse, T.: The  
 381 atmospheric role in the Arctic water cycle: A review on processes, past and future changes, and their impacts, *J. Geophys. Res.*  
 382 *Biogeosci.*, 121, 586– 620, doi:10.1002/2015JG003132, 2016.  
 383 Walczowski, W., Beszczynska-Möller, A., Wieczorek, P., Merchel, M., and Grynczel, A.: Oceanographic observations in the  
 384 Nordic Sea and Fram Strait in 2016 under the IO PAN long-term monitoring program AREX, *Oceanologia*, 59(2), 187-194,  
 385 doi:10.1016/j.oceano.2016.12.003, 2017.  
 386 Wawrzyniak, T., Osuch M., Napiórkowski, J.J., and Westerman, S.: Modelling of the thermal regime of permafrost during  
 387 1990–2014 in Hornsund, Svalbard. *Polish Polar Research* 37(2): 219–242, doi: 10.1515/popore-2016-0013, 2016.  
 388 Wawrzyniak, T., Osuch, M., Nawrot, A., and Napiórkowski, J.J.: Run-off modelling in an Arctic unglaciated catchment  
 389 (Fuglebekken, Spitsbergen). *Ann. Glaciol.* 58 (75), 36–46, doi:10.1017/aog.2017.8, 2017.  
 390 Wawrzyniak, T., Osuch, M.: A consistent High Arctic climatological dataset (1979-2018) of the Polish Polar Station Hornsund  
 391 (SW Spitsbergen, Svalbard). *PANGAEA*, <https://doi.pangaea.de/10.1594/PANGAEA.909042>, 2019.  
 392 Wojkowski, J., Caputa, Z., and Leszkiewicz, J.: The impact of relief on the diversity of possible sunshine duration at Hornsund  
 393 region (SW Spitsbergen), *Problemy Klimatologii Polarnej* 25, 179-190, 2015.